

# **Self-waveguided photoemission with high efficiency and self-cavity lasing of organic crystalline wires made by improved epitaxial growth method**

Shusuke Kanazawa, Musubu Ichikawa,\* Toshiki Koyama and Yoshio Taniguchi

[a] Dr. M. Ichikawa, Mr. S. Kanazawa, Prof. T. Koyama, Prof. Y. Taniguchi

Department of Functional Polymer Science, Faculty of Textile Science and Technology, Shinshu University, 3-15-1 Tokita, Ueda 386-8567 (Japan)

Fax: (+81)268-21-5413

E-mail: musubu@shinshu-u.ac.jp

**Keywords:** laser, organic semiconductor, epitaxial growth, thiophene oligomer, photoluminescence

Recently, thin films of conjugated molecules as active materials in electronic, optoelectronic and photonic devices have received great attention.<sup>[1, 2]</sup> Growths of highly oriented crystalline materials are of particular interest because these materials improve electronic and photonic properties. Therefore, it is promised that organic devices such as thin film transistors, light-emitting diodes and solid-state lasers based on organic materials attain higher performance.<sup>[1, 3-6]</sup> Furthermore, the ability to prepare highly controlled molecular alignments in nano-space will lead to organic nanotechnology in future. In this paper we describe a preparation of highly oriented molecular crystalline wires of  $\alpha$ ,  $\omega$ -di(biphenyl)-*ter*thiophene (BP3T; see Fig. 1a) by an improved epitaxial growth technique and their characteristic photonic properties: self-waveguided photoemissions with a high internal quantum efficiency and self-cavity lasing. Oligothiophene and its derivatives are a promising candidate for electronic, optoelectronic and photonic applications because these compounds intrinsically possess superior charge-transporting properties compared with oligophenylene like *para*-sexiphenyl that is representative ring assembled oligomers, due to stronger intermolecular interactions based on large atomic radius of sulfur.<sup>[7, 8]</sup> In addition, oligothiophenes exhibit good photo and electroluminescence and stimulated emission properties with high quantum efficiency in crystalline state compared with oligoacene like pentacene that is another  $\pi$ -conjugated oligomers having out-standing charge-transporting natures.<sup>[9-11]</sup> As generally known a longer thiophene sequence leads to higher luminescence performance and color varieties. However, there is no report on epitaxial growth, which is a potential method to prepare highly oriented molecular crystalline materials on a substrate,<sup>[12-16]</sup> for thiophene derivatives containing three or more repetitions of thiophene units, to the best of our knowledge. As mentioned above, here we demonstrate the epitaxial preparation of highly oriented molecular crystalline wires and the characteristic photonic properties of BP3T.

Figure 1b shows a fluorescence microscope image of BP3T crystals grown on a freshly cleaved KCl (001) face by using an improved vapor phase epitaxial growth technique that utilizes argon as a buffer gas. The pressure of argon was -60 kPa against the atmosphere. The crystals are like wires, which are totally along to the directions of

[110] or  $[1\bar{1}0]$  of the KCl (001) face. Dimensions of the wires were typically several hundreds  $\mu\text{m}$  long, a few  $\mu\text{m}$  wide and a few  $\mu\text{m}$  high, respectively.

According to previously reported literatures on other wire-like epitaxially grown materials such as *para-sexiphenyl* and other thiophene/phenylene co-oligomers with smaller thiophene contents than BP3T,<sup>[4, 13, 17, 18]</sup> molecules align parallel against the KCl surface and perpendicularly to the wire long direction. The similar orientation in the case of BP3T was confirmed with the X-ray diffraction (XRD) pattern of the BP3T wires shown in Figure 2a. The XRD pattern shows two reflections at  $2\theta$  of  $21.4^\circ$  ( $d = 4.1 \text{ \AA}$ ) and  $23.7^\circ$  ( $d = 3.76 \text{ \AA}$ ). Hollows at  $2\theta$  of around  $6^\circ$  and  $12^\circ$  arise from elastomer used for a sample preparation. According to the crystal parameters of BP3T previously reported,<sup>[19]</sup> the  $3.76\text{-\AA}$ -spacing strong reflection agrees with the half-length of the *a*-axis. This confirms that the *bc*-plane of the wire crystals contacts with the KCl surface. In addition, the BP3T crystalline wires disappeared when the wires were observed with the fluorescence microscope through a parallel polarizer (analyzer) against the wire long axis. Since the *c*-axis is approximately parallel to the molecular long axis as shown in Figure 2b, the BP3T crystalline wires were grown along the *b*-axis of BP3T crystal. Note that since there is no reflection related to  $b/2$ , the needles are just grown along the *b*-axis. On the other hand, the other reflection at  $21.4^\circ$  could not be related to any crystal parameter of BP3T.<sup>[19]</sup> At present we consider that a part of epitaxially grown wire crystals near the KCl surface has different lattices due to the lattice mismatch between KCl and BP3T. Anyway, the molecular orientation in the wire-like crystals of BP3T was fully consistent with the other reported epitaxially grown wire-like molecular crystals such as *para-sexiphenyl* and other thiophene/phenylene co-oligomers with shorter thiophene sequence. Longer thiophene sequence probably causes higher functionality that results from strong intermolecular interactions based on larger atomic size of sulfur. To the best of our knowledge, this is the first report on the epitaxially grown crystals of the molecular materials with *ter*thiophene. This vapor phase epitaxial growth with inert buffer gas at the optimal pressure led to this achievement. In fact, quite different morphology appeared at other argon pressures as shown in Figure 1c.

As clearly shown in Fig. 1b, the crystalline wires show bright

photoluminescence. As mentioned before, BP3T molecules align in perpendicular to the wire direction and in parallel to the substrate KCl surface. Since the transition dipole moment is along to the molecular long axis, photoluminescence from BP3T molecules preferentially radiates in a plane consisting of the wire direction vector and the normal vector of the substrate surface. In addition, the crystalline wires work as ridge waveguides. Therefore, self-waveguided photoemission should be observed. As we can see from Figure 1b, there are some bright light spots at the wire end faces. This clearly ensures the self-waveguided photoemission effect of the crystals.

The intense photoemission from BP3T crystalline wires suggests that the radiative transition process in BP3T crystal is completely allowed and faster than other competing processes such as internal conversions and intersystem crossing. Figure 3a shows the photoemission intensity decay profile from BP3T crystalline wires observed around 575 nm. A peak in the negative time region arises from a weak pre-pulse of the laser. The luminescence at overall wavelength totally decayed in accordance with single exponential behavior at the same lifetime of 1.68 ns. This short lifetime is comparable with that of highly efficient laser dyes such as comarines, rhodamines, DCM derivatives and so on. The similar fast single exponential behavior was also observed at other temperatures from 300 K to 60 K. Note that another spectrum assigned to phosphorescence was not observed at 60 K at all. Figure 3b shows the temperature dependence of the photoluminescence lifetimes of BP3T crystalline wires. The lifetime increased with decreasing temperature, but the increasing seemed to be saturated below 100 K. The initial increasing results from suppressing non-radiative transition processes that are usually thermally activated. Because the lifetime became to be approximately constant below 100 K, the thermally activated non-radiative transition processes will be prohibited at the low temperature.

As mentioned above, there was no phosphorescence from the crystals at 60 K, and the fluorescence lifetimes were almost saturated at the temperature. These findings strongly indicate that intersystem crossing in this material is negligible. Therefore, we analyzed the temperature dependence of the fluorescence lifetime with the well known following equation with no intersystem crossing term:<sup>[20]</sup>

$$\tau(T) = 1 / (k_f + k_{nr}^0 \exp(-\Delta E / k_B T)), \quad (1)$$

where  $\tau$ ,  $k_f$ ,  $k_{nr}^0$ ,  $\Delta E$ ,  $k_B$  and  $T$  represented the fluorescence lifetime, the radiative transition rate constant, the frequency factor and the activation energy of the non-radiative transition, the Boltzman constant and the temperature, respectively. As Figure 3b also showed the best fitting result, Eq. (1) fully analyzed the temperature dependence. The parameters at the best fitting were:  $k_f = 4.8 \times 10^8 \text{ s}^{-1}$ ,  $k_{nr} = 1.2 \times 10^8 \text{ s}^{-1}$ ,  $\Delta E = 50 \text{ meV}$ . We estimated an *internal* fluorescence quantum efficiency from the lifetime and these parameters; thus, the quantum efficiency at 300 K was estimated to be 0.80. In addition, as we will point out after, BP3T crystals have high durability against intense photoexcitations without any sensitivities to ambient conditions of moistures and oxygen. The high efficiency and durability show that BP3T crystal is a promising material for photonics and optoelectronics based on organic materials.

Next, we would like to discuss optical amplification behavior in BP3T crystals. As mentioned before, BP3T molecules aligned in perpendicular to the wire axis and the crystalline wires show the self-waveguide effect for the photoluminescence. These features effectively work for optical amplification by stimulated emission. Figure 4a shows self-waveguided photoemission spectra from BP3T crystalline wires at intense ( $43.8 \mu\text{J cm}^{-2}$ ) and weak ( $5.5 \mu\text{J cm}^{-2}$ ) excitation conditions. Note that PL intensity did not decrease after the intense pumping over several hundred laser-shots in the atmosphere. The photoemission spectrum under the intense pumping was considerably narrow than that under the weak excitation. This spectrally narrowed photoemission will result from gain-narrowing based on stimulated emission. Furthermore, as shown in Fig. 4b, a sharp peak abruptly appeared at an excitation density of  $19.0 \mu\text{J cm}^{-2}$  at the same wavelength of the spectrally narrowed photoemission above-mentioned. The intensity of this “sharp peak” increased without any narrowing, while the broad spontaneous emission spectrum was superimposed. This behavior strongly suggests that the spectrally narrowed photoemission results from laser oscillation not amplified spontaneous emission. In addition, the inset of Fig. 4a shows the high resolution PL spectrum of the narrowed spectrum shown in Fig. 4a. There are several peaks with approximately equal intervals, which means a presence of a Fabry-Pérot resonator in pathway of the emission. The resonator length ( $L$ ) was estimated from peak interval ( $\Delta\lambda$ ), wavelength ( $\lambda$ ) and index of refraction ( $n$ ) with Equation (2):<sup>[21]</sup>

$$L \approx \frac{\lambda^2}{2n \cdot \Delta\lambda} \quad (2).$$

The values of  $\lambda$  and  $\Delta\lambda$  were, respectively, 572.94 nm and  $0.26 \pm 0.02$  nm from the inset of Fig. 4a. Hence, we obtained  $L \approx (640 \pm 60)/n$   $\mu\text{m}$ . Since a refractive index of organic materials usually ranges from *ca* 1.5 to 2, the resonator length is supposed to be 300 ~ 400  $\mu\text{m}$ . Because this length corresponded to only the length of the wires, it was shown that both end edges of the wires acted as optical mirrors. Thus, the crystalline wires work for not only waveguides but also optical resonators. In other words, the almost equally split spectrum, namely, the spectrally narrowed photoemission resulted from self-cavity lasing. Finally, briefly note that the propagation loss constant at the wavelength of the fluorescence maximum was evaluated to be 0.074 dB  $\mu\text{m}^{-1}$  from the analysis of the self-waveguided photoemission of the wires. The loss constants increased at shorter wavelength and decreased at longer, and then became  $\sim 0$  dB  $\mu\text{m}^{-1}$  above 585 nm. This means that the loss probably results from optical absorptions of the crystal itself.

In summary, we have successfully fabricated epitaxially grown crystals of BP3T on KCl (001) faces using the improved vapor phase growth technique that is expected to be applicable to various organic materials. The BP3T crystals were like wires along to [110] or  $[\bar{1}\bar{1}0]$  of the KCl (001) face. The BP3T crystalline wires emitted bright self-waveguided photoemission from the wire edges with the high internal quantum PL efficiency. The efficiency at 300 K was estimated to be 0.8. The spectrally narrowed self-waveguided photoemission was observed under intense photopumping. The almost equally split PL spectrum and the pumping intensity dependence of the PL spectra around the *threshold* indicated that the spectrally narrowed photoemission arose from the self-cavity lasing effect of the BP3T crystals. Thus, the epitaxially grown BP3T crystalline wire is a promising material for organic photonics and optoelectronics.

## Acknowledgments

This work was supported by the Cooperative Link for Unique Science and Technology for Economy Revitalization (CLUSTER) of the Japan's Ministry of Education, Culture,

Sports, Science and Technology. It was also supported by the Ministry's 21st Century COE program.

## **Experimental**

The synthesis and purification procedures for BP3T can be found elsewhere.<sup>[22]</sup> Vapor phase growth of BP3T crystals was carried out in a semi-closed cylindrical quartz cell placed in a home made sealed chamber. A freshly cleaved KCl single crystal (Furuuchi Chemical) was placed at the top of the quartz cell with face-down setting, and source materials were loaded at the bottom of the cell. While argon was charged in the chamber as an inert buffer gas, the semi-closed cell was also filled argon because buffer gases easily move in and out the cell through small clearances between the cylindrical cell and a side end cap made of quartz. The cell was placed in a cylindrical bore furnace fixed in but thermally isolated from the chamber. The furnace has a controllable temperature gradient from the bottom (higher temperature) to the top (lower temperature). Crystals took about 24 hours to grow in the chamber. The charge pressure of Ar changed from -20 to -80 kPa against the atmosphere.

Photoluminescence dynamics of the growth crystals was measured with a Hamamatsu Photonics streak scope photon counting system (C4780) coupled with a second harmonic light (392.5 nm) of a femtosecond (pulse duration: 110 fs) laser (Thales Lasers, Bright). A sample: crystals on a KCl substrate, was set in a cryostat to change temperatures from 60 K to 300 K. Laser pulses to pump the sample were sufficiently attenuated to be 31.0 nJ/cm<sup>2</sup>/pulse to avoid nonlinear deactivations. The excitation intensity dependence of photoemission behavior of the crystals was measured using a nitrogen gas laser (pulse duration: 500 ps) as an intense light source and a high resolution spectrograph composed of an  $f=750$  mm polychromator with 100 or 1200 lines/mm blazed grating and a charge-coupled device camera (Andor, DV420-OE). The maximum resolution of the spectrograph is 26 pm. Fluorescence microscope photographs were taken with a Nikon ECLIPSE E600. XRD patterns were measured using Cu  $K\alpha$  radiation with the  $\theta/2\theta$  geometry. Samples for measuring XRD were prepared as follows: 1) cast silicone elastomer (Dow corning, SILPOT 184 W/C) on KCl substrate to capture grown crystals, 2) remove KCl with pure water after curing for

24 hours at room temperature. Optical propagation losses of single crystalline wire were evaluated with an in-house modified multipurpose microscope (WITec, AlphaSNOM). An objective lens (x 20) focused excitation light from a semiconductor laser ( $\lambda = 405$  nm) excited a small part of the single crystalline wire, and then a spectrograph, which consisted of an Oriel 77480 polychromator and an Andor DH520-18U-01 CCD camera, recorded self-waveguided photoemissions from an end-edge as a function of distances between the excitation part and the edge.

### **References**

- [1] C. D. Dimitrakopoulos, P. R. L. Malenfant, *Adv. Mater.* **2002**, *14*, 99.
- [2] S. R. Forrest, *Nature* **2004**, *428*, 911.
- [3] J. Fraxedas, *Adv. Mater.* **2002**, *14*, 1603.
- [4] M. Ichikawa, H. Yanagi, Y. Shimizu, S. Hotta, N. Suganuma, T. Koyama, Y. Taniguchi, *Adv. Mater.* **2002**, *14*, 1272.
- [5] E. Menard, V. Podzorov, S.-H. Hur, A. Gaur, M. E. Gershenson, J. A. Rogers, *Adv. Mater.* **2004**, *16*, 2097.
- [6] M. Ichikawa, R. Hibino, M. Inoue, T. Haritani, S. Hotta, K.-i. Araki, T. Koyama, Y. Taniguchi, *Adv. Mater.* **2005**, *17*, 2073.
- [7] H. E. Katz, A. Dodabalapur, Z. Bao, *Oligo- and Polythiophene-Based Field-Effect Transistors*, (Wiley-WCH, Weinheim, **1998**).
- [8] G. Horowitz, M. E. Hajlaoui, R. Hajlaoui, *J. Appl. Phys.* **2000**, *87*, 4456.
- [9] H. Klauk, M. Halik, U. Zschieschang, G. Schmid, W. Radlik, W. Weber, *J. Appl. Phys.* **2002**, *92*, 5259.
- [10] T. W. Kelley, L. D. Boardman, T. D. Dunbar, D. V. Muyres, M. J. Pellerite, T. P. Smith, *J. Phys. Chem. B* **2003**, *107*, 5877.
- [11] V. C. Sundar, J. Zaumseil, V. Podzorov, E. Menard, R. L. Willett, T. Someya, M. E. Gershenson, J. A. Rogers, *Science* **2004**, *303*, 1644.
- [12] H. Yanagi, T. Morikawa, *Appl. Phys. Lett.* **1999**, *75*, 187.
- [13] H. Yanagi, T. Morikawa, S. Hotta, K. Yase, *Adv. Mater.* **2001**, *13*, 313.
- [14] A. Andreev, G. Matt, C. J. Brabec, H. Sitter, D. Badt, H. Seyringer, N. S. Sariciftci, *Adv. Mater.* **2000**, *12*, 629.
- [15] S. Lukas, S. Sohnchen, G. Witte, C. Woll, *ChemPhysChem* **2004**, *5*, 266.

- [16] G. Koller, S. Berkebile, J. R. Krenn, G. Tzvetkov, G. Hlawacek, O. Lengyel, F. P. Netzer, C. Teichert, R. Resel, M. G. Ramsey, *Adv. Mater.* **2004**, *16*, 2159.
- [17] H. Yanagi, T. Ohara, T. Morikawa, *Adv. Mater.* **2001**, *13*, 1452.
- [18] H. Yanagi, Y. Araki, T. Ohara, S. Hotta, M. Ichikawa, Y. Taniguchi, *Adv. Funct. Mater.* **2003**, *13*, 767.
- [19] S. Hotta, M. Goto, R. Azumi, M. Inoue, M. Ichikawa, Y. Taniguchi, *Chem. Mater.* **2004**, *16*, 237.
- [20] N. Mataga, T. Kubota, *Molecular interaction and electronic spectra*, (Marcel Dekker, New York, **1970**) chapter 4.
- [21] A. Yariv, in *Quantum Electronics*, (John Wiley & Sons, New York **1989**), p.145.
- [22] S. Hotta, T. Katagiri, *J Heterocyclic Chem.* **2003**, *40*, 845.

### Figure Captions

Figure 1. (a) Structural formula of BP3T and fluorescence micrographs of epitaxially grown crystals of BP3T at -60 kPa (b) and -80 kPa (c).

Figure 2. (a) XRD pattern of grown crystals of BP3T, (b) unit cell of BP3T.

Figure 3. (a) PL decay profile of the BP3T crystalline wires measured at 300 K, and (b) temperature dependence of the PL lifetimes of the BP3T crystals. Solid line shows the theoretical fitting result (see text).

Figure 4. (a) PL spectra of BP3T crystalline wires under the weak (dotted line) and the intense (solid line) excitation. The inset shows high-resolution PL spectrum of BP3T under the intense excitation. (b) PL spectra at several excitation intensities around  $19.0 \mu\text{J cm}^{-2}$ .

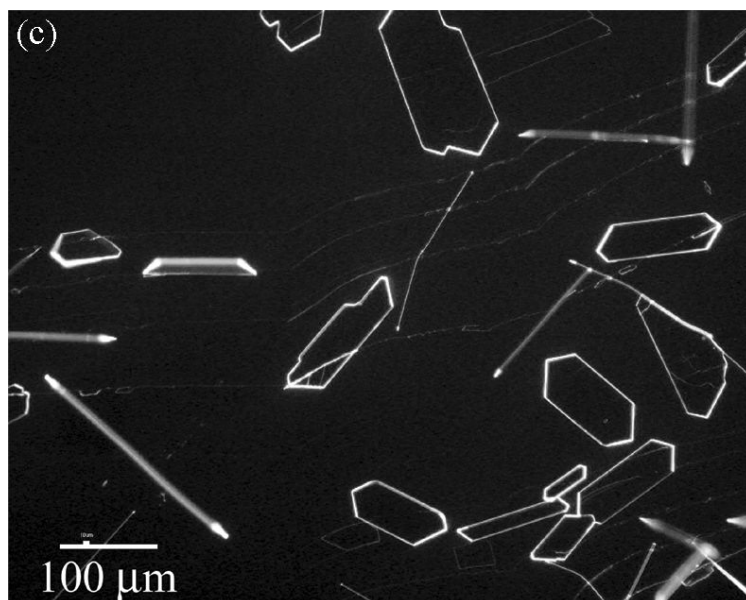
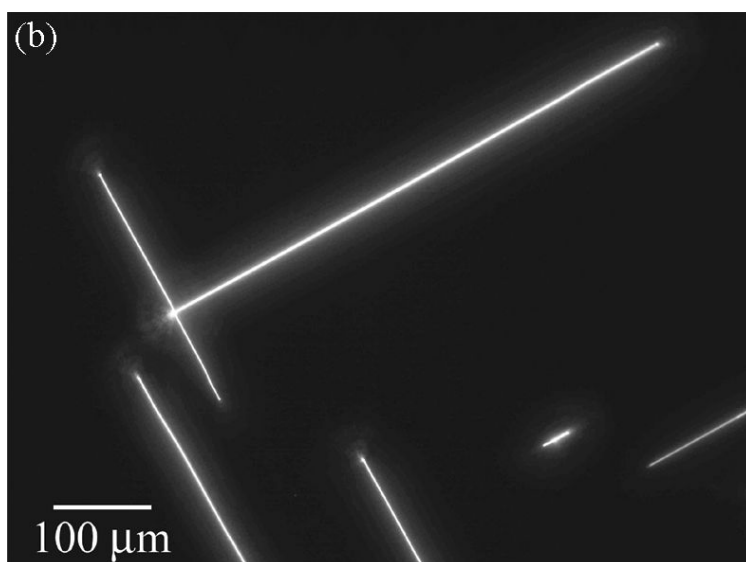
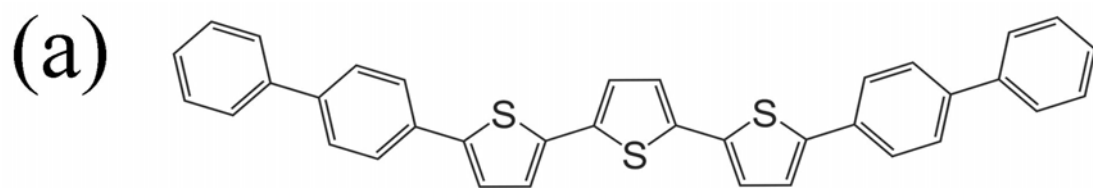


Figure 1

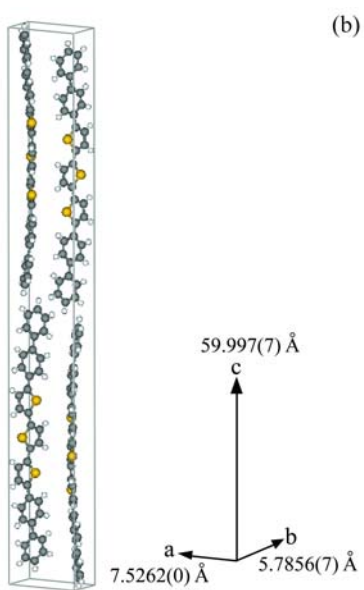
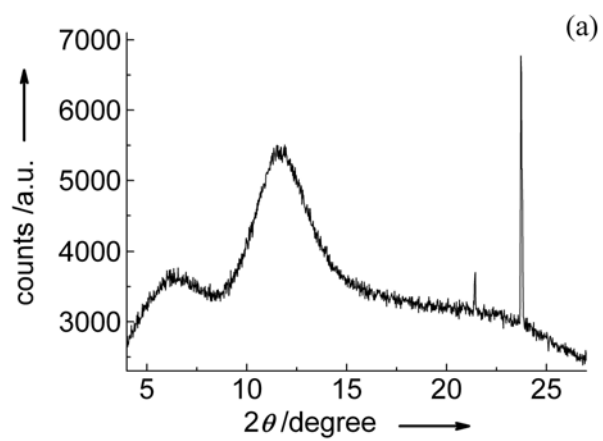


Figure 2

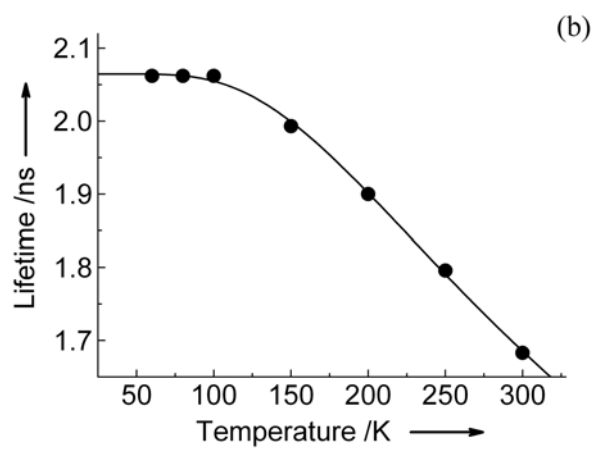
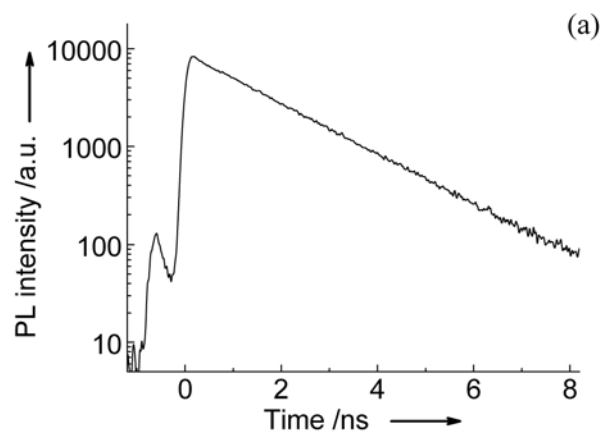


Figure 3

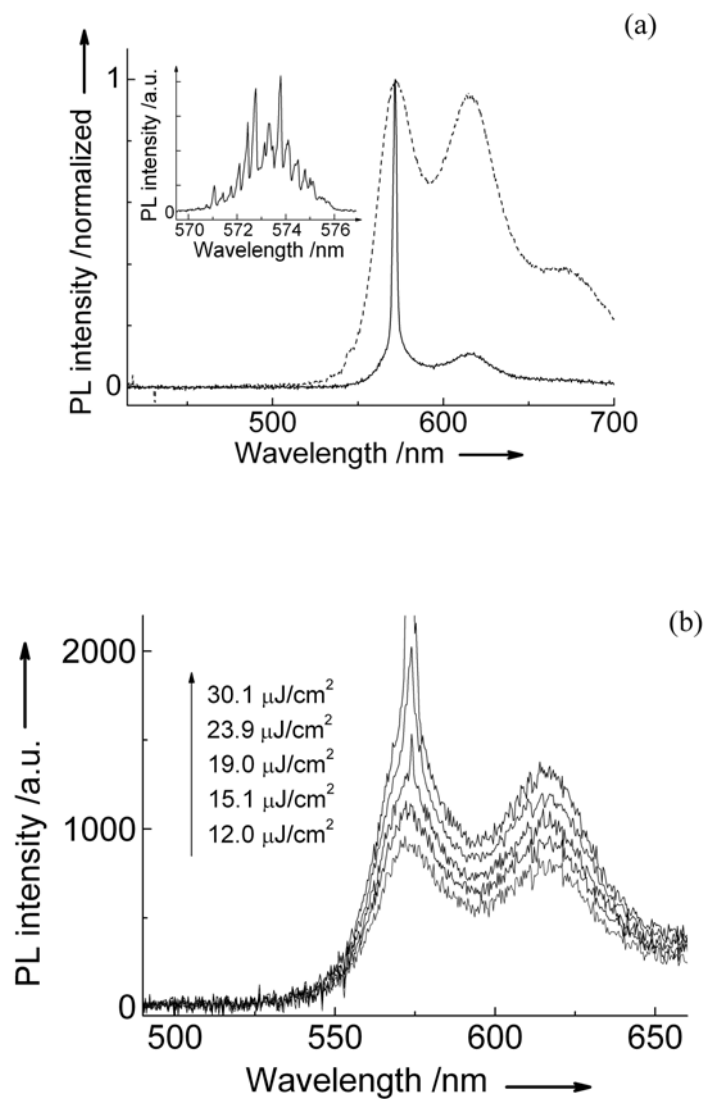


Figure 4